TRANSVERSE RESISTIVE WALL IMPEDANCE FOR MULTI-LAYER FLAT CHAMBERS

Alexey Burov and Valeri Lebedev, FNAL

Abstract

The transverse resistive wall impedance is calculated for arbitrary multi-layer vacuum chambers with a flat geometry. A finite thickness of the metal layer is important at impedance calculations for long machines like VLHC [1], thin coating of elements like injection kickers [2] and a closed orbit coherent stability analysis [3]. This paper uses ideas of our similar consideration for round vacuum chambers [4].

1 METHOD OF CALCULATION

For non-round vacuum chambers, there are three transverse impedances: driving vertical, driving horizontal and detuning [5]. The two driving impedances describe dipole fields caused by beam offsets. The detuning impedance describes quadrupole fields awoken by the beam current; this impedance has the same value and opposite signs for the two transverse degrees of freedom. For a flat geometry, the detuning impedance is exactly equal to the horizontal driving impedance due to the horizontal homogeneity. Thus, only two driving impedances has to be found in this case.

Calculations of the electromagnetic fields excited by the beam dipole motion are significantly simplified when it is realized that the wave length of the beam transverse oscillations is much longer than the half-gap, $c/\omega \gg a$, which is always true as soon as the finite skin depth plays a role. Charges and currents excited on the chamber surface feel only local beam offset; thus, they feel the beam as moving in parallel to the chamber axis with small transverse oscillations at a given frequency ω.

This beam motion can be presented as a superposition of oscillating electric and magnetic dipoles: one is due to the beam charge and another due to its current [1]. The chamber response on the electric dipole is simply electrostatic screening. For the electrostatic response, only the transverse electric field $\vec{E} = -\nabla\Phi$ is non-zero; it can be found from the scalar potential Φ excited by the beam offset inside an ideally conducting vacuum chamber. The potential is found from the 2D transverse Laplas equation:

$$\nabla^2\Phi = 0\,, \tag{1}$$

with zero boundary conditions on the chamber surface $\Phi|_\Gamma = 0$.

A response on the vertical beam oscillations has to be found assuming that the beam has a charge dipole moment $Iy_0/(\beta c)$. Thus, the total potential can be presented as a direct contribution of the beam dipole, $\Phi_b = Iy_0 y/(\beta c r^2)$, with βc as the beam velocity, and a reaction of the vacuum chamber, Φ_c; thus, $\Phi = \Phi_b + \Phi_c$, where Φ_c is a regular function satisfying the Laplas equation.

The oscillating magnetic dipole gives rise to the transverse magnetic field. Due to a fact that the longitudinal wave length is much larger than the aperture, this field can be expressed through the longitudinal vector potential A. In the vacuum, the vector potential satisfies the same Laplas equation (1) as the scalar one, and also can be presented as a sum of the direct beam contribution and the chamber reaction: $A = A_b + A_c$ with $A_b = \Phi_b\beta$ and A_c. as a regular harmonic function.

The scalar potential can be also expressed as $\Phi = A^\infty/\beta$, where A^∞ is the solution for the vector potential at infinite conductivity, $A^\infty|_\Gamma = 0$.

Using A. Chao's convention [6], the vertical impedance per unit length

$$Z_y = -i(E_y + \beta H_x)/(Iy_0) \tag{2}$$

can be written as

$$Z_y = \frac{-i\beta}{Iy_0}\left(\frac{\partial A_c}{\partial y} - \frac{1}{\beta^2}\frac{\partial A_c^\infty}{\partial y}\right)\Bigg|_{r\to 0}\,. \tag{3}$$

Note that in this definition the direct dipole contributions A_b, Φ_b are excluded.

The impedance (3) can also be expressed as a sum of an ideal-conductivity term $Z^\infty \propto \beta^-1\gamma^{-2}$ and a term caused by the wall resistivity $Z^\sigma \propto (A - A^\infty)$:

$$Z_y \equiv Z_y^\sigma + Z_y^\infty = \frac{-i\beta}{Iy_0}\left(\frac{\partial(A_c - A_c^\infty)}{\partial y} - \frac{1}{\beta^2\gamma^2}\frac{\partial A_c^\infty}{\partial y}\right)\Bigg|_{r\to 0}\,. \tag{4}$$

The horizontal Fourier transformation is used to solve the Laplas equation:

$$\hat{A} = \int_{-\infty}^{\infty} A\exp(-ikx)dx \tag{5}$$

From the Laplas equation, the Fourier image inside the vacuum chamber follows:

$$\hat{A} = D(e^{-|ky|} - G_y(k)\sinh(ky)e^{-|k|a}/\sinh(ka))\,, \tag{6}$$

where $D = 2\pi Iy_0/c$ and the inner metal plates are assumed at $a \le |y| \le a + d$. A first term in the brackets, $\propto e^{-ky}$, is the Fourier image of the beam dipole field A_b. The second term describes the chamber potential A_c, and the introduced amplitude $G_y(k)$ has to be found from the boundary conditions. This amplitude is defined here so that for infinite conductivity, $A(a) = 0$, $G_y(k) = 1$. Substitution of this Fourier image into the impedance definition (4) leads to

$$Z_y^\infty = -i\frac{Z_0}{2\pi\beta\gamma^2}\int_0^\infty dk\frac{ke^{-ka}}{\sinh ka} = -i\frac{Z_0}{2\pi a^2\beta\gamma^2}\frac{\pi^2}{12}\,, \tag{7}$$

$$Z_y^\sigma = -i\frac{Z_0\beta}{2\pi}\int_0^\infty dk\frac{ke^{-ka}}{\sinh ka}(1-G_y(k))\,. \qquad (8)$$

Similar considerations for the horizontal beam oscillations give

$$\hat{A} = -iD\frac{k}{|k|}\left(e^{-|ky|} - G_x(k)\cosh(ky)\frac{e^{-|k|a}}{\cosh(ka)}\right) \quad (9)$$

$$Z_x^\infty = -i\frac{Z_0}{2\pi\beta\gamma^2}\int_0^\infty dk\frac{ke^{-ka}}{\cosh ka} = -i\frac{Z_0}{2\pi a^2\beta\gamma^2}\frac{\pi^2}{24} \qquad (10)$$

$$Z_x^\sigma = -i\frac{Z_0\beta}{2\pi}\int_0^\infty dk\frac{ke^{-ka}}{\cosh ka}(1-G_x(k)) \qquad (11)$$

$$Z_x = Z_x^\infty + Z_x^\sigma\,. \qquad (12)$$

Inside a medium with a conductivity σ and a magnetic permeability μ, the vector potential satisfies the 2D quasi-static equation

$$\nabla^2 A - \kappa^2 A = 0 \qquad (13)$$

with

$$\kappa^2 = -\frac{\omega^2\mu}{c^2}(1+\frac{4\pi i\sigma}{\omega})\,. \qquad (14)$$

which means $\kappa^2 = -2i/\delta^2$ with δ as the skin-depth inside a metal.

In terms of the horizontal Fourier components,

$$\hat{A} = D\,(C\,\cosh(q(y-a)) + S\,\sinh(q(y-a))) \qquad (15)$$

for the vertical oscillations and with a minor change $D \to -iD$ for horizontal. Here a is the coordinate of the inner surface of the given layer and $q = \sqrt{\kappa^2+k^2}$.

The free field amplitudes $G_{x,y}(k)$ in Eqs. (8,11) (and so the impedances) can be found after continuity conditions on A and $\mu^{-1}dA/dy$ are imposed at any layer's boundary. An additional condition at infinity, $\lim_{y\to\infty}\hat{A} = 0$ leads to the field expression in the outermost medium:

$$\hat{A}_o \propto e^{-q|y|}\,, \qquad (16)$$

assuming $\mathrm{Re}\,q > 0$. Altogether, the presented equations lead to an analytic expression for the impedance for any number of layers. For a flat geometry, this expressions have a structure similar to the round case [4], with an obvious complication: they are expressed as integrals over the horizontal wave vectors k. The integrals, however, are regular and fast converging at $ka \gg 1$.

In the next section, the impedances are found for an arbitrary two-layer structure, with a metallic layer inside and an arbitrary unbounded medium outside.

2 TWO-LAYER CHAMBER

In this section, the impedance is found for an arbitrary two-layer chamber with a flat symmetry. It is convenient here to use a subscripts $1, 2$ for values related to the first or second layer and introduce $\tilde{q} \equiv q/\mu = \sqrt{\kappa^2+k^2}/\mu$ as a "medium parameter".

For the vertical oscillations, the continuity conditions for $\hat{A}$ and $\mu^{-1}d\hat{A}/dy$ at $y = a$ and $y = a+d$ are expressed as

$$\begin{gathered}\exp(-ka)(1-G_y) = C\\ -\exp(-ka)(1+G\coth(ka)) = S\tilde{q}_{10}\\ Cc_1 + Ss_1 = G_o\\ Cs_1 + Sc_1 = -G_o\tilde{q}_{21}\end{gathered} \qquad (17)$$

for $k > 0$. Here $c_1 = \cosh(q_1 d)\,,\ s_1 = \sinh(q_1 d)$; the parameters $\tilde{q}_{10} \equiv \tilde{q}_1/\tilde{q}_0 \equiv \tilde{q}_1/k$ and $\tilde{q}_{21} \equiv \tilde{q}_2/\tilde{q}_1$ reflect relative properties of adjacent media, and the constant G_o describes vector potential in the outer layer.

Making a ratio from the first pair of the boundary equations leads to an expression of the impedance factor $1-G_y$ in terms of the amplitude ratio $T = S/C$:

$$1 - G_y = (1+\coth(ka))/(\coth(ka) - \tilde{q}_{10}T)\,. \qquad (18)$$

Similarly, a pair of equations at the outer boundary leads to a solution for the amplitude ratio T:

$$T = -(\tilde{q}_{21} + t_1)/(1 + \tilde{q}_{21}t_1) \qquad (19)$$

with $t_1 = \tanh(q_1 d)$. Substitution Eq. (19) into Eq. (18) leads to

$$1 - G_y = \frac{(1+\tilde{q}_{21}t_1)\exp(ka)}{c_0 + \tilde{q}_{21}\tilde{q}_{10}s_0 + (\tilde{q}_{21}c_0 + \tilde{q}_{10}s_0)t_1} \qquad (20)$$

with $c_0 = \cosh(ka)\,,\ s_0 = \sinh(ka)$.

Corresponding results for the horizontal (x) oscillations follows from the vertical (y) ones (18, 20) by an interchange $s_0 \leftrightarrow c_0$; thus,

$$1 - G_x = \frac{(1+\tilde{q}_{21}t_1)\exp(ka)}{s_0 + \tilde{q}_{21}\tilde{q}_{10}c_0 + (\tilde{q}_{21}s_0 + \tilde{q}_{10}c_0)t_1}\,. \qquad (21)$$

Substitution of the amplitudes (20, 21) in the impedance expressions (8, 11) and integration over the horizontal wave number k leads to the final result. The integrals cannot be evaluated analytically in general case, but they can be for some specific cases. Anyway, their numerical evaluation is straightforward: the integrals are regular and fast converging $\propto \exp(-2ka)$ at $ka \gg 1$.

When the inside metal is non-magnetic and the outside media is vacuum, the vertical impedance (8) can be presented as

$$Z_y^\sigma \simeq -i\frac{Z_0\beta}{2\pi a^2}\int_0^\infty d\xi\frac{\xi^2}{\sinh\xi(\xi e^\xi + \tau\sinh\xi)}\,, \qquad (22)$$

where $\tau = \kappa a\tanh(\kappa d)$, and $|\kappa|a \gg 1$, which normally covers the whole interesting area of parameters. Then, the integral here can be approximated as

$$\int_0^\infty d\xi\frac{\xi^2}{\sinh\xi(\xi e^\xi + \tau\sinh\xi)} \approx \frac{\pi^2}{12}\frac{1}{1+\tau/2}\,, \qquad (23)$$

with an accuracy better than 5% for arbitrary $0 \le \tau \le \infty$. Thus,

$$Z_y^\sigma = -i\frac{\pi^2}{12}\frac{Z_0\beta}{2\pi a^2}\frac{1}{1+\tau/2}\,, \qquad (24)$$

which is a factor of $\pi^2/12$ smaller than the impedance of a similar round chamber with a radius a.

Same considerations lead to the horizontal impedance

$$Z_x^\sigma = -i\frac{\pi^2}{24}\frac{Z_0\beta}{2\pi a^2}\frac{1}{1+\tau/2}\,, \qquad (25)$$

with the accuracy 13% or better for any value of τ. This accuracy gets to be absolute for $\tau \gg 1$.

Note that the same form-factors $\pi^2/12$ and $\pi^2/24$ describe the ideal conductivity impedances of the flat chamber in comparison with the round one:

$$Z_y^\infty = \frac{\pi^2}{12}Z_{\rm round}^\infty\,, \quad Z_x^\infty = \frac{\pi^2}{24}Z_{\rm round}^\infty\,. \qquad (26)$$

If the outside medium is a low-conductive magnetic ($\sigma_1 \gg \sigma_2\,,\ \mu_2 \gg 1$), the same values of the form-factors are exactly correct at $\tau \equiv \kappa a\tanh(\kappa d) \gg 1$. For more details, the impedances are shown in Fig. (1) in units of $Z_0\beta/(2\pi a^2)$ as functions of $ad/\delta^2 \propto \omega$. While at high frequencies, $ad/\delta^2 \gg 1$, the vertical impedance dominates over the horizontal, $Z_y^\sigma = 2Z_x^\sigma$, at low frequencies it is not so any more: $\mathrm{Re}(Z_y^\sigma)/\mathrm{Re}(Z_x^\sigma) \propto \sqrt{ad}/\delta \ll 1$. The impedances are independent of the outer layer when $\sqrt{\sigma_2/\mu_2} \ll \sqrt{\sigma_1/\mu_1}\tanh(\kappa_1 d)$.

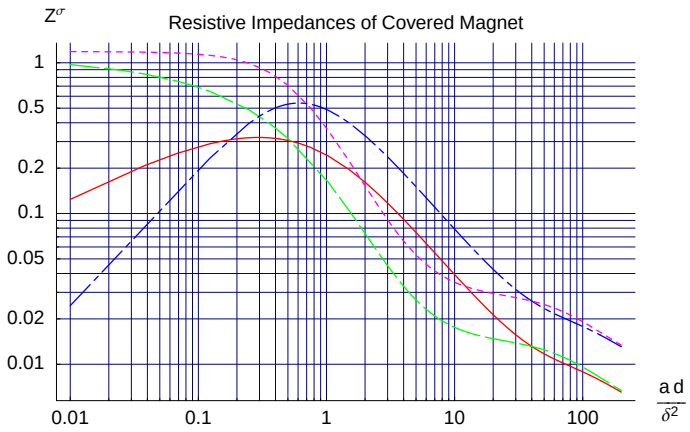

Figure 1: Impedances of a two-layer vacuum chamber, metal inside and a low-conductive magnetic outside. Impedances are shown in units of $Z_0/(2\pi a^2)$, as functions of $ad/\delta^2 \propto \omega$. Solid red and dashed green lines give real and negated imaginary parts of the horizontal impedance, dash-dotted blue and dotted magenta lines are same for the vertical. Calculations are performed for $d/a = 0.05\,,\ \mu_1 = 1,\ \mu_2 = 500,\ \sigma_2/\sigma_1 = 0.1$.

This two-layer chamber can be compared with a single material one, when the magnetic metal is not covered by the non-magnetic conductor at all. The impedances of such flat homogeneous magnetic resistive walls are shown in Fig. (2).

While the vertical scales for the two cases are approximately equal, the horizontal ones are normally very different. For the homogeneous magnetic chamber, the

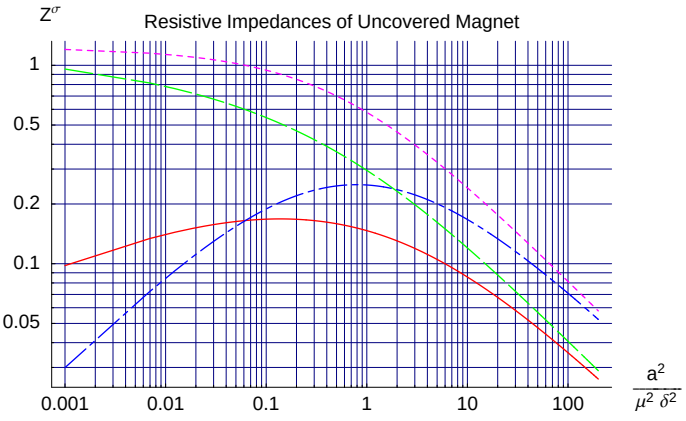

Figure 2: Impedances of flat thick (uncovered) magnetic walls with $\mu = 500$, in units of $Z_0/(2\pi a^2)$, as functions of $a^2/(\mu^2\delta^2) \propto \omega/\mu$. The lines have similar meaning as for Fig. (1). Calculations for the both figures are performed with *Mathematica* [7]

impedances are located at $\omega \le \omega_\mu = \mu c^2/(2\pi\sigma a^2) \propto \mu$ and slowly go down as $\sqrt{\omega_c/\omega}$ at higher frequencies. Instead, when the non-magnetic conductor covers this magnet, the frequency range can be significantly shrunk: the impedances are mainly at $\omega \le \omega_2 = c^2/(2\pi\sigma ad) \propto a/d$ and fall faster, $\propto \omega_2/\omega$, at higher frequencies.

If the number of layers is more than 2, the described solution can be obviously generalized in the same way as it is done for the round geometry [4].

3 CONCLUSIONS

For flat geometry of multi-layer vacuum chambers, the resistive impedances can be calculated in the same way as they are for the round case [4]. A method of calculations is described and applied for a two-layer structure. Several limit cases are discussed in details.

4 REFERENCES

[1] V. Lebedev, "Multi-Bunch Instabilities in VLHC", presented in VLHC Workshop, SLAC, March 2001.

[2] V. Danilov, S. Henderson, A. Burov and V. Lebedev, "An Improved Impedance Model of Metallic Coating", Proc EPAC'02.

[3] A. Burov, V. Danilov, Phys. Rev. ST-AB **4**, 120101 (2001).

[4] A. Burov, V. Lebedev, "Transverse Resistive Wall Impedance for Multi-Layer Round Chambers", Proc. EPAC'02.

[5] A. Burov, V. Danilov, Phys. Rev. Lett. **82**, 2286 (1999).

[6] A. W. Chao, "Physics of Collective Beam Instabilities in High Energy Accelerators", J. Wiley & Sons, Inc, 1993.

[7] S. Wolfram, "Mathematica", Addison-Wesley, 1991. Our nb file is at www-bdnew.fnal.gov/pbar/organizationalchart/lebedev/Articles/index.htm.